JP4.4 ROLES OF LAND USE AND OROGRAPHY ON THE SIMULATED SUMMER MONSOON OVER SOUTH ASIA USING A REGIONAL CLIMATE MODEL

Suhee Park and Song-You Hong*
Department of Atmospheric Sciences, Yonsei University, Seoul, Korea

1. Introduction

It is well known that the Asian summer monsoon is an extremely complex phenomenon that encompasses variabilities over a wide range of spatial and temporal scales (e.g., Lau et al. 2000). Prediction of the monsoon is one of the major challenges of climate research (Schubert and Wu 2001; Basu 2001; Douville et al. 2001; Douville 2002; Liu et al. 2002). It has been recognized by a number of observational studies that the Asian monsoon system, of which the Indian summer monsoon is a major component, plays an important role as a major energy source in the global-scale circulation in middle and low latitudes (e.g., Parthasarathy et al. 1991).

Most of previous studies about the role of land properties in the Indian summer monsoon were conducted by using general circulation models (GCMs) or simple models (Hahn and Manabe 1975 ; Sashegyi and Greisler 1987; Mawson and Cullen 1992; Fennessy et al. 1994; Laval et al. 1996; Chakraborty et al. 2003). Hahn and Manabe (1975) and Chakraborty et al. (2003) showed that mountains have an important effect on the onset and temporal variations of the Indian monsoon. Laval et al. (1996) showed that when vegetation is not represented in the model the model does not simulate accurately the interannual variation of the precipitation rates. Fennessy et al. (1994) performed experiments to test the sensitivity of the Indian monsoon simulation to change in orography, vegetation, soil wetness, and cloudiness. They found that the role of orography is most important in realistic simulation of Indian monsoon circulation and rainfall.

There is a limitation to understand mechanisms responsible for Indian monsoon using GCMs. One is the predictability problem. Another limitation is due to a coare-resolution of the GCMs covering the globe. To circumvent the resolution problem in GCMs, the regional climate modeling (RCM) approach has been actively utilized. In addition to the usage of downscaling of climate signals resolved in low-resolution global models, the facts that the large-scale circulation is forced to remain realistic by the use of reanalysis boundary conditions, and that the regional model provides no feedback to the large-scale, allow isolating the regional feedbacks, something very difficult to attain within the standard approach of global model integrations (Hong and Kalnay 2000).

In this paper, the role of land properties, such as vegetation fractions, vegetation types, soil types, land-sea contrast, and orography, in the simulation of Indian monsoon using a RCM are investigated. The model description and experimental design are presented in section 2. The results from the sensitivity experiments are discussed in section 3. Concluding remark are given in section 4.

2. Model and Experimental design

The National Centers for Environmental Prediction (NCEP) regional spectral model (RSM) has been widely used in the virtues of its unique features including the domain-nesting strategy and perturbation method. The RSM is a primitive equation model using the sigma-vertical coordinate. A detailed model description is given by Juang et al. (1997) and Hong and Leetmaa (1999). Land processes physics utilizes Oregon State University (OSU) two-layer soil model (Pan 1990; Chen and Dudhia 2001). In the OSU model, land surface evaporation consists of three components: direct evaporation from the bare soil surface, transpiration through the leaf stomatae, and evaporation of precipitation intercepted by the leaf canopy.

The RSM domain (45-115 E, 16S-40N) covers the South Asian monsoon region, which includes the Indian Ocean, South East Asia, and the southern part of the Tibetan Plateau (Fig. 1). The number of grid points in Cartesian coordinates is 129 (west-east) by 110 (north-south). A 60-km resolution is chosen so that the RSM captures meso-α scale features embedded in the planetary-scale monsoon system. Initial conditions and large-scale forcing were obtained from the NCEP-NCAR Reanalysis data (Kalnay et al. 1996).

Four runs are designed to investigate the role of land use properties and orography in the simulation of Indian monsoon (Table 1). The CNTL experiment uses land surface data set from the U.S. Geological Survey (Chen and Dudhia 2001). The variables are the vegetation fraction, the vegetation type, and soil type. The USGS soil and vegetation categories are classified as 16 and 13, respectively. The vegetation fraction ranges from 0 to 100 %. Following experiments change an option from the

* *Corresponding author address*: Song-You Hong, Yonsei University, Dept. of Atmospheric Sciences, Seoul, Korea; e-mail: shong@yonsei.ac.kr

Table 1. A summary of experiments.

	Land surface conditions			Land-sea contrast	Orography
	Vegetation fraction	Vegetation type	Soil type		
CNTL	variable	variable	variable	yes	yes
HOMO	70%	meadow and shrub land	Sandy clay loam	yes	yes
LD2SEA	variable	variable	variable	no	yes
NOMNT	variable	variable	variable	yes	no

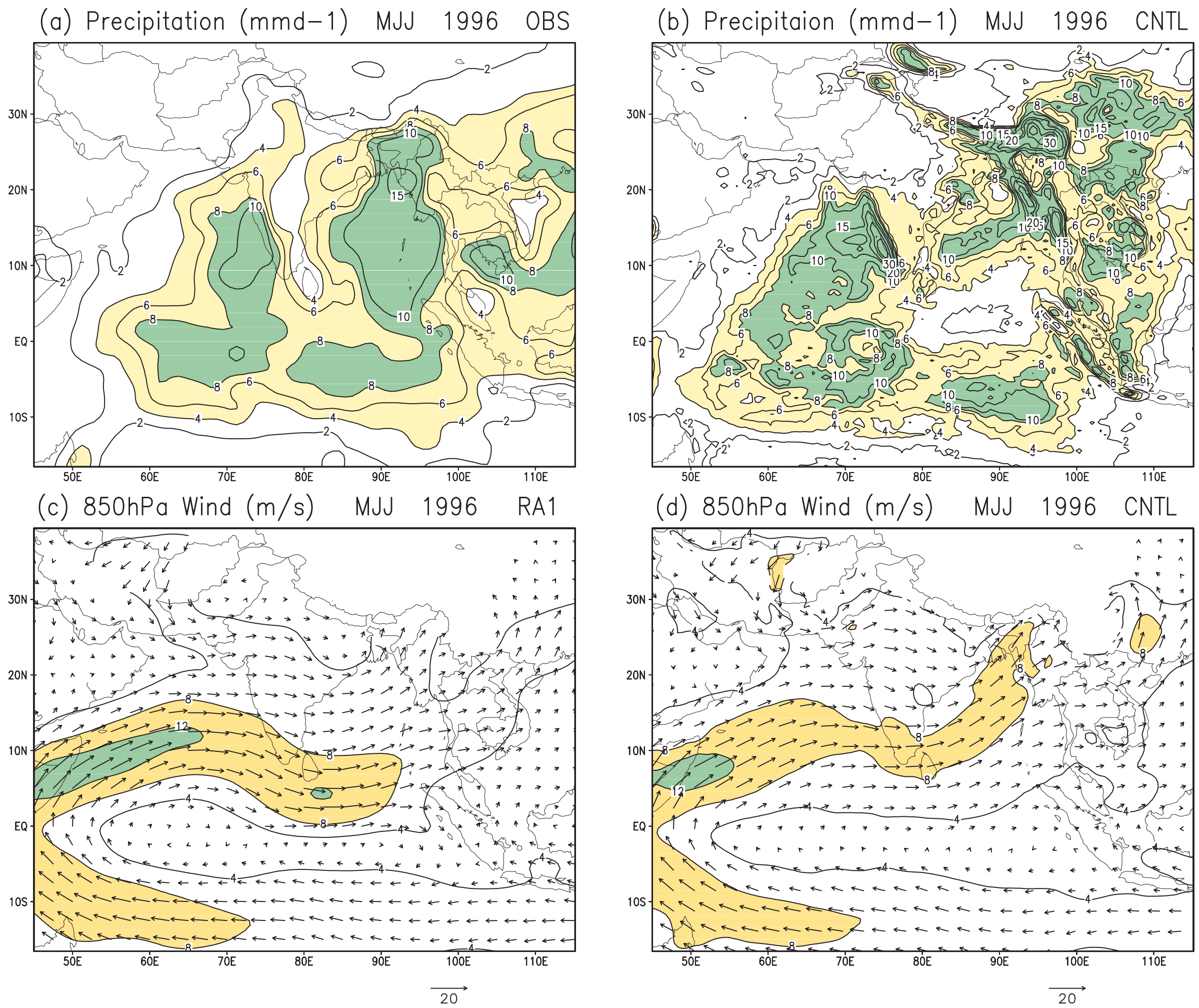

Fig. 1. Seasonal mean (May-June-July) precipitation intensity (mmd^{-1}) and 850hPa wind (ms^{-1}) of the observation and the CNTL experiment (CMAP for observed precipitation and NCEP-NCAR reanalysis for wind)

CNTL experiment. The HOMO experiment uses homogeneous surface conditions such as vegetation type with meadow and shrub land, vegetation fraction with 70%, and soil type with sandy clay loam. In the LD2SEA experiment, land areas over the model domain are replaced by water points. In other words, the values of vegetation type and soil type over land points changed to be the values over water. In the NOMNT experiment, entire land region is set to flat plain as the height being nearly zeros, except for the boundary buffer zones.

3. Results and Discussion

Overall, the control simulation reproduces the precipitation and large-scale features very well in terms of seasonal mean as well as intra-seasonal variability. The model reproduces well observed rainfall and the low-level circulation associated with the summer monsoon over India (Fig. 1). Four rainfall peaks which locate in the Bay of Bengal, Arabian Sea just west of Indian continent, and southern Indian Oceans centered at 72 E and 85 E are well captured by model. These maxima are typical pattern of the Indian summer monsoonal rainfall. The model results exhibit some details related to orography distribution, for example, a peak at the western flank of the Indian continent. Note that high detailed features in precipitation is absent in the CMAP analysis due to a 2.5 degree resolution. However, simulated precipitation intensity is larger than the observation. Precipitation averaged over the whole domain of the CNTL experiment and observation is 4.94 and 4.64 mmd^{-1}, respectively (Table 2).

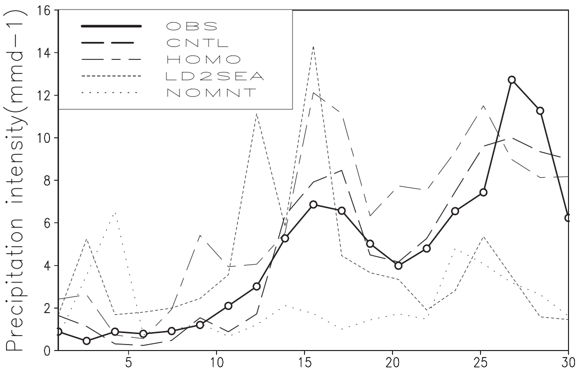

Fig. 2. Time series of Pentad mean precipitation intensity (mmd^{-1}) averaged over the India continental region (8.4-28.0N, 68.2-90.7E, land only), obtained from the CMAP and experiments.

The associated large-scale circulation is well produced (Fig. 1c and 1d). The low-level inter-hemispheric gyre circulation characterized by easterlies over the southern Indian Ocean (about 10S), connected via the Somali jet to the westerlies across the Indian subcontinent, is well simulated, although the westeries are weakened in the model. This feature is dynamically consistent with precipitation pattern in Figure 1b, which is reported in previous studies (Krishnamurti 1985, Lau et al. 2000). Simulated intra-seasonal variability of precipitation is also good. The model reproduces well the evolution of summer monsoon precipitation over India (Fig. 2).

The HOMO experiment with the homogeneous land surface conditions generally increases the precipitation (Fig. 3a). The cyclonic low-level circulations over the Arabian Sea and the Bay of Bengal are seen clearly. It seems to be due to the increment of land-sea contrast. Because in this experiment land surface is uniform, the contrast between land surface and sea surface is strengthened. For the whole integration period, precipitation increased, compared with the CNTL

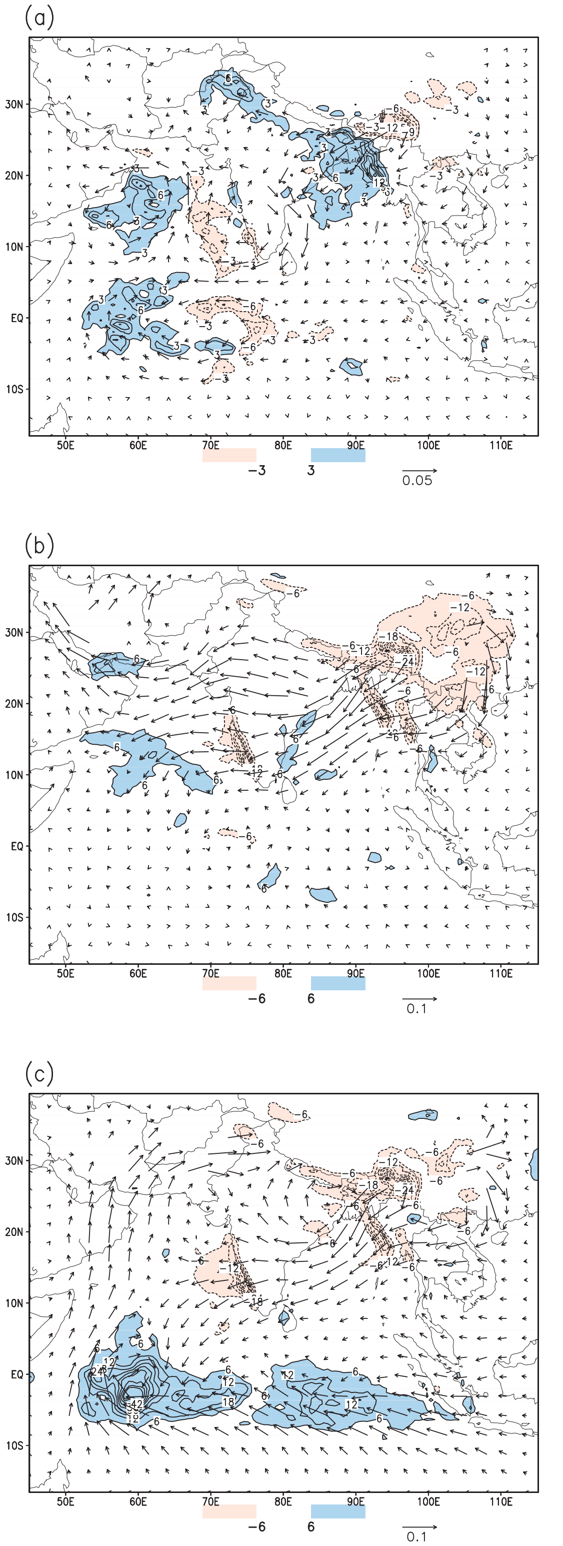

Fig. 3. The differences of precipitation intensity (mmd^{-1}, shaded) and 850hPa moisture flux (kgkg^{-1}ms^{-1}, vector) between the CNTL experiment and (a) the HOMO, (b) the LD2SEA, and (c) the NOMNT experiment. Note that contour intervals for precipitation and flux vector in (b) and (c) are doubled over that in (a).

Table 2. Statistics of MJJ mean precipitation from experiments, which include mean, biases, RMS errors, and pattern correlation coefficients over whole domain, and temporal correlations of pentad precipitation averaged over India continental region with the CMAP data.

	MJJ mean (mmd^{-1})	**Bias** (mmd^{-1})	**RMS Error** (mmd^{-1})	**Pattern Correlation**	**Temporal Correlation**
CNTL	4.94	0.30	2.24	0.63	0.93
HOMO	5.21	0.57	2.43	0.62	0.78
LD2SEA	4.72	0.08	2.52	0.58	0.12
NOMNT	5.97	1.33	3.53	0.48	0.19

experiment (Fig. 2). It confirms above explanation. It is not straightforward to examine the role of soil and vegetation type for each category. However, we may say that the correct representation of the soil and vegetation types in model plays an important role in simulating the intra-seasonal variability of monsoon rainfall as well as seasonal mean precipitation. It is noted that the pattern and temporal correlation of the HOMO experiment are less than those of the CNTL experiment (Table 2).

The effect of land-sea contrast over the Indian region on the summer monsoon is more significant than the effects due to land use properties seen above (Fig. 3b). Overall, seasonal mean precipitation is enhanced except for South East Asian region. Removal of land portion reduces westerlies in inter-hemispheric gyre circulation by weakening land-sea contrast, enhances the moisture flux convergence in south and western part, and diminishes the moisture flux transport in north and eastern part. The strong moisture flux convergence leads to intense rainfall over Arabian Sea and the Bay of Bengal region and reduced moisture flux transport leads to reduction of precipitation over southern China and Indo-China region. Increase of precipitation over Indian region for May and June is due to large evaporation over water which is larger than land. Reduction of precipitation in July seems to be due to a dynamical effect of reduced pressure gradient between land and ocean with time (Fig. 2). Seasonal mean precipitation over India decreases because precipitation variation for July is prevailed.

The impact of orography on monsoon rainfall is prominent in the low-level inter-hemispheric gyre circulation (Fig. 3c). Increase of precipitation between Equator and 10 S is significant, and the corresponding easterly anomalies in that area are clearly visible. Similarly, precipitation over land is reduced, and corresponding weakening of westeries around the Bay of Bengal is visible, too. It is interesting to note that the major change of circulation is limited to the north of 10 N when l land points are replaced by water points, whereas the removal of orogaphy weakens inter-hemispheric gyre monsoonal circulation significantly.

Table 2 is statistics of the RSM experiments. It can be seen that RMS error, Pattern correlation and temporal correlation increase consistently from the CNTL experiment to the NOMNT experiment. The results have shown that the effect of orography is more important than land-sea contrast.

4. Concluding remarks

We have described the effect of land use properties and orography on the Indian summer monsoon simulated by a regional climate model. The model was integrated for the period 1 May – 31 July 1996, driven by reanalysis data. By comparing the results with the control experiment, the features of sensitivity experiments have been investigated.

It is found that the correct representation of land surface conditions in model plays an important role in simulating the intra-seasonal variability of monsoon rainfall as well as seasonal mean precipitation. Also, it can be seen that the land-sea contrast enhances westeries north of 10 N, which plays a principal role in transporting the moisture flux to India and southern china region. Meanwhile, orography not only enhanced westeries north of 10 N, but also weakens easteries south of equator. It is interesting to note that orography affects the whole inter-hemispheric gyre circulation. It may be due to that the dynamical forcing of orography to the monsoon circulation is greater than the forcing of the land-sea contrast.

Acknowledgements. This research was supported by the Climate Environment System Research Center sponsored by the SRC program of Korea Science and Engineering Foundation

REFERENCES

Basu, B. K., 2001: Simulation of the Summer Monsoon over India in the Ensemble of Seasonal Simulations from the ECMWF Reanalyzed Data. *J. Climate*, 14, 1440–1449.

Chakraborty, A., R. S. Nanjundiah and J. Srinivasan, 2002: Role of Asian and African orography in Indian summer monsoon. *Geophys. Res. Lett.,* 29, 10.1029/2002GL015522.

Chen, Fei, and Jimy. Dudhia, 2001a: Coupling an

Advanced Land Surface–Hydrology Model with the Penn State–NCAR MM5 Modeling System. Part I: Model Implementation and Sensitivity. *Mon. Wea. Rev.,*129, 569–585.

______, and ______, 2001b: Coupling an Advanced Land Surface–Hydrology Model with the Penn State–NCAR MM5 Modeling System. Part II: Preliminary Model Validation. *Mon. Wea. Rev.,* 129, 587–604.

Douville, H., F. Chauvin, and H. Broqua, 2001: Influence of Soil Moisture on the Asian and African Monsoons. Part I: Mean Monsoon and Daily Precipitation. *J. Climate*, 14, 2381–2403.

______, 2002: Influence of Soil Moisture on the Asian and African Monsoons. Part II: Interannual Variability. *J. Climate*, 15, 701–720.

Fennessy, M.J., J. L. Kinter, B. Kirtman, L. Marx, S. Nigam, E. Schneider, J. Shukla, D. Straus, A. Vernekar, Y. Xue, and J. Zhou, 1994: The Simulated Indian Monsoon: A GCM Sensitivity Study. *J. Climate*, 7, 33–43.

Hahn, Douglas G. and Syukuro Manabe, 1975: The Role of Mountains in the South Asian Monsoon Circulation. *J. Atmos. Sci.* 32, 1515–1541.

Hong, S.-Y., and Ants Leetmaa, 1999: An Evaluation of the NCEP RSM for Regional Climate Modeling. *J. Climate,* 12, 592–609.

_________, and Eugenia Kalnay, 2002: The 1998 Oklahoma-Texas Drought: Mechanistic Experiments with NCEP Global and Regional Models. *J. Climate,* 15, 945-963.

Juang, H.-M. H., S.-Y. Hong, and M. Kanamitsu, 1997: The NCEP regional spectral model: An update. *Bull. Amer. Meteor. Soc.*, 78, 2125-2143.

Kalnay, E., and Coauthors, 1996: The NCEP/NCAR 40-year reanalysis project. *Bull. Amer. Meteor. Soc.*, 77, 437-471.

Krishnamurti, T. N., 1985: Summer Monsoon Experiment—A Review. *Mon. Wea. Rev.* 113, 1590–1626.

Lau, K.-M., K.-M. Kim, and S. Yang, 2000: Dynamical and Boundary Forcing Characteristics of Regional Components of the Asian Summer Monsoon. *J. Climate*, 13, 2461–2482.

Laval, K., R. Raghava, J. Polcher, R. Sadourny, and M. Forichon, 1996: Simulations of the 1987 and 1988 Indian Monsoons Using the LMD GCM. *J. Climate*, 9, 3357–3372.

Liu, Yimin, Johnny C. L. Chan, Jiangyu Mao, and Guoxiong Wu, 2002: The Role of Bay of Bengal Convection in the Onset of the 1998 South China Sea Summer Monsoon, *Mon. Wea. Rev.*, 130, 2731-2744.

Mawson, M. H., and M. J. P. Cullen, 1996: An idealized simulation of the Indian monsoon using primitive-equation and quasi-equilibrium models, *Q. J. R. Meteorol. Soc.*, 118, 153-164.

Pan, Hua-Lu, 1990: A Simple Parameterization Scheme of Evapotranspiration over Land for the NMC Medium-Range Forecast Model. *Mon. Wea. Rev.*, 118, 2500–2512.

Parthasarathy, B., K. Rupa Kumar, and A. A. Munot, 1991: Evidence of Secular Variations in Indian Monsoon Rainfall–Circulation Relationships. *J. Climate*, 4, 927–938.

Sashegyi, Keith D. and John E. Geisler, 1987: A Linear Model Study of Cross-Equatorial Flow Forced by Summer Monsoon Heat Sources. *J. Atmos. Sci.* 44, 1706–1722.

Schubert, Siegfried D. and Man Li Wu, 2001: Predictability of the 1997 and 1998 South Asian Summer Monsoon Low-Level Winds. *J. Climate,* 14, 3173–3191.